

Summertime tropospheric ozone variability over the Mediterranean basin observed with IASI

C. Doche^{1*}, G. Dufour¹, G. Foret¹, M. Eremenko¹, J. Cuesta¹, M. Beekmann¹, and P. Kalabokas^{2,3}

¹Laboratoire Inter-universitaire des Systèmes Atmosphériques (LISA), Universités Paris-Est Créteil et Paris Diderot, CNRS, Créteil, France

²Academy of Athens, Research Center for Atmospheric Physics and Climatology, Athens, Greece

³European Commission, JRC, Institute for Environment and Sustainability, Air and Climate Unit, Ispra, Italy

*Now at Météo France, Direction Inter-Régionale Sud-Ouest, Division Etudes et Climatologie, Mérignac, France

Correspondence to: C. Doche
(clement.doche@meteo.fr)

Abstract. The Mediterranean basin is one of the most sensitive regions of the world regarding climate change and air quality. This is partly due to the singular dynamical situation of the Mediterranean basin that leads to among the highest tropospheric ozone concentrations over the Northern Hemisphere. Six years of summertime tropospheric ozone observed by the Infrared Atmospheric Sounding Interferometer (IASI) instrument from 2007 to 2012 have been analysed to document the variability of ozone over this region. The satellite observations have been examined together with meteorological analyses (from ECMWF) to understand the processes driving this variability. Our work confirmed the presence of a steep West-East ozone gradient in the lower troposphere with the highest concentrations observed over the Eastern part of the Mediterranean basin. This gradient is mainly explained by diabatic convection over the Persian Gulf during the Indian Monsoon season, which induces an important subsidence of ozone rich air masses from the upper to the lower troposphere over the central and the Eastern Mediterranean basin. IASI observations of ozone concentrations at 3 km height show a clear summertime maximum in July that is well correlated to the maximum of downward transport of rich-ozone air masses from the upper troposphere. Even if this feature is robust over the six analyzed years, we have also investigated monthly ozone anomalies, one positive (June 2008) and one negative (June and July 2009) using daily IASI observations. We show that the relative position and the strength of the meteorological systems (Azores anticyclone and Middle Eastern depression) present over the Mediterranean are key factors to explain both the variability and the anomalies of ozone in the lower troposphere in this region.

20 1 Context and problematic

Lower tropospheric ozone (O_3) is a harmful pollutant for both human health and vegetation (Levy et al., 2001; Fuhrer, 2009). In the upper troposphere, ozone acts as a powerful greenhouse gas (IPCC, 2007). The presence of ozone throughout the troposphere depends on the meteorological conditions driving vertical and horizontal transport and on photochemical ozone production from its precursors
25 (mainly nitrogen oxides NO_x and volatile organic compounds VOCs; Delmas et al., 2005; Camredon and Aumont, 2007; Jacob, 2000). Well documenting and understanding the ozone variability is both crucial with respect to climate change and air quality (Volz-Thomas et al., 2003).

The Mediterranean basin is sensitive to both climate change and atmospheric pollution, mainly during summer. Indeed, climate change experts expect an intensification of the summertime dryness
30 (IPCC, 2007) which is already typical for this region. The combination of the specific meteorological conditions prevailing during summer and the regional air pollution emissions produce an enhancement of lower tropospheric ozone concentrations over this area (Nolle et al., 2001; Lelieveld et al., 2002; Kalabokas and Repapis, 2004; Velchev et al., 2011). These summertime meteorological conditions are characterised by two high pressure ridges, one over the Central Europe and one over
35 the Western Mediterranean basin, and a deep trough extending from the Persian Gulf to the Eastern Mediterranean basin (Fig. 1a). The Central Europe ridge results from an extension of the Azores anticyclone, while the Western ridge results from an extension of the North African anticyclone. These systems lead to low winds, persistent clear sky conditions, and high solar irradiation over the Mediterranean (Prezerakos, 1984; Tyrlis and Lelieveld, 2013; Anagnostopoulou et al., 2014).

40 The Eastern trough is associated to the strong convection linked to the summertime Indian monsoon (Fig. 1b; for further information see also Alpert et al., 2005). Indeed, the ascending motion induced by the Indian monsoon produces a cellular circulation, which leads to strong descending winds just over the Central and Eastern Mediterranean. This corresponds to one of the strongest occurrences of subsidence over the entire Northern hemisphere (about $0.15 \text{ Pa}\cdot\text{s}^{-1}$ in the South of Greece, see
45 Fig. 1b and also Ziv et al., 2004). In addition, a lower tropospheric North-South circulation, referred as Etesian winds, occurs over the Central Mediterranean basin between these two meteorological systems (eastward of Greece; Ziv et al., 2004). These meteorological conditions favor 1) the horizontal transport of polluted air masses, with potentially high ozone concentrations, from Eastern continental Europe to the Mediterranean Sea (Kalabokas et al., 2008; Richards et al., 2013) and 2)
50 the vertical downward transport of ozone-enriched air masses from the upper troposphere and the lower stratosphere. Moreover, the persistence of anticyclonic conditions, associated with high solar irradiation and low winds, can induce photochemical ozone production within the plumes of the densely urbanized areas located along the Mediterranean coasts, although the regional background ozone levels are generally more important (Kalabokas and Repapis, 2004).

55 Over the Eastern Mediterranean basin, the presence of an ozone pool in the middle troposphere has been noticed by several observational and modeling studies (e.g., Marengo et al., 1998; Stohl

et al., 2001; Jonson et al., 2001; Li et al., 2001; Roelofs et al., 2003; Liu et al., 2009; Zanis et al., 2014). Most of these studies suggest that this ozone pool is likely produced by downward transport from the upper troposphere and lower stratosphere. In addition, the impact of European emissions on ozone concentrations over the Eastern basin within the boundary layer has been estimated by Richards et al. (2013) and this contribution remains limited. Kalabokas et al. (2013) show that high ozone concentrations in the lower troposphere are related to anticyclonic events, which reinforce subsidence and the Etesian advection of potentially ozone-enriched air masses coming from Europe. Following these authors, low ozone concentrations in the lower troposphere are related to cyclonic conditions, characterized by advection of oceanic ozone poor air masses from the Atlantic to the Mediterranean. These studies are mainly based on accurate in-situ observations from ozone-sondes or MOZAIC/IAGOS vertical profiles and surface stations – (Kalabokas et al., 2013; Zbinden et al., 2013) but their specific geographic and temporal sampling only provide an incomplete vertical description of the troposphere over the entire basin. Model simulations have been used by Richards et al. (2013) and Zanis et al. (2014) to describe the tropospheric ozone distribution, although their coarse resolution may induce large uncertainties.

To complement these model and in situ measurements approaches, satellite observations provide interesting opportunities. Indeed, in the last decade, satellite observations of tropospheric ozone have been developed and have become more and more precise (e.g., Fishman et al., 2003; Liu et al., 2005; Coheur et al., 2005; Worden et al., 2007; Eremenko et al., 2008). These observations are now able to complement in situ observations offering large spatial coverage and good horizontal resolution. Thermal infrared nadir sounders like the Tropospheric Emission Spectrometer (TES) instrument (Beer et al., 2001) aboard EOS-AURA and the Infrared Atmospheric Sounding Interferometer (IASI) instrument aboard MetOp (Clerbaux et al., 2009) provide a maximum of sensitivity in the mid-troposphere with an effective vertical resolution of about 6-7 km and have been used to study atmospheric composition and transport, climate and air quality (e.g., Worden et al., 2008; Jones et al., 2008; Eremenko et al., 2008; Boynard et al., 2009; Dufour et al., 2010; Safieddine et al., 2013). Richards et al. (2013) and Zanis et al. (2014) have used ozone observations derived from TES and/or GOME-2 to confirm the presence of the ozone pool over the Eastern Mediterranean basin. In the present study, ozone observations derived from IASI measurements using the approach developed by Eremenko et al. (2008) are used to document the spatiotemporal variability of lower and upper tropospheric ozone over the Mediterranean basin during summertime. One advantage of IASI with respect to TES is that IASI's scanning capacity offers a quasi-global coverage twice a day with dense horizontal sampling (pixels spaced by 25 km at nadir). Moreover, compared to UV sounders, IASI measurements exhibit much better sensitivity to lower tropospheric ozone concentrations (Cuesta et al., 2013; Foret et al., 2014). In the present study, six years of IASI observations are analysed and compared to meteorological reanalyses from the ECMWF ERA-Interim model in order to evaluate the role on the atmospheric dynamical processes for the tropospheric ozone distribution

and its variability over the Mediterranean basin. This study complements previous studies adding a
95 new independent set of observations with relatively fine horizontal resolution and good sensitivity
for lower tropospheric ozone. The very large number of individual IASI measurements, allows us
to conduct month-to-month analyses (for summer periods) over the Mediterranean in the lower free
troposphere (around 3 km altitude) and to focus on ozone anomalies analyses with respect to the
climatological mean on a daily scale.

100 The IASI ozone observations used for the present study are described in section 2 as well as the
meteorological data and the analysis method. In section 3, summertime spatiotemporal variability
of ozone over the Mediterranean basin is analysed in parallel with meteorological conditions for the
2007-2012 period. From this analysis, two tropospheric ozone anomalies with respect to the clima-
tological evolution are identified in June 2008 and June/July 2009. They are discussed in section 4.
105 Conclusions are given in section 5.

2 Ozone observations and methodology

2.1 IASI measurements of tropospheric ozone

2.1.1 The IASI instrument

The IASI instrument (Clerbaux et al., 2009) on board of the MetOp-A platform since 19 October
110 2006 is a nadir-viewing Fourier transform spectrometer operating in the thermal infrared between
645 and 2760 cm^{-1} with a (apodized) spectral resolution of 0.5 cm^{-1} . The IASI field of view
is composed of a 2×2 matrix of pixels with a diameter at nadir of 12 km each. IASI scans the
atmosphere with a swath width of 2200 km allowing monitoring atmospheric composition twice a
day at any (cloud free) location. The spectral coverage and the radiometric and spectral performances
115 of IASI allow this instrument to measure the global distribution of several important atmospheric
trace gases (e.g., Boynard et al., 2009; George et al., 2009; Clarisse et al., 2011). Concerning ozone,
3 to 4 pieces of information are available for the overall retrieved profile depending on the thermal
conditions. In the troposphere, up to 1.5 degrees of freedom are observed under favourable thermal
conditions. In particular, Dufour et al. (2010) have shown the ability to capture separately the ozone
120 variability in the lower and upper troposphere under summer conditions, thus enabling its use for air
quality studies in polluted regions.

2.1.2 Ozone retrieval

The ozone profiles considered in the present study are retrieved using the method described in Ere-
menko et al. (2008). These IASI ozone observations are well validated and characterized (Keim et
125 al., 2009; Dufour et al., 2012). Briefly, the retrievals are based on the radiative transfer model KO-
PRA (Karlsruhe Optimized and Precise Radiative transfer Algorithm, Stiller et al. (2000)) and its

inversion module KOPRAFIT (Hopfner et al., 2001). A constrained least squares fit method using an analytical altitude-dependent regularization is used (Kulawik et al., 2006). The applied regularization method is detailed in Eremenko et al. (2008). Compared to previous studies using this algorithm (Eremenko et al., 2008; Dufour et al., 2010, 2012), a selection between two a priori ozone profiles has been added and is based on the detection of the tropopause height. Tropopause height is calculated from the temperature profile retrieved from IASI using the definition based on the lapse rate criterion (WMO, 1957). A threshold (14 km) has been selected for choosing as well the a priori and the regularization matrix. If the tropopause height is lower (higher) than 14 km, a constraint and a priori typical for mid-latitudes (tropics) are used. The regularization matrices are those already used in Eremenko et al. (2008) for the mid-latitudes and in Dufour et al. (2010, 2012) for the tropics. The a priori profiles used during the retrieval are compiled from the climatology of McPeters et al. (2007). The mid-latitude a priori profile is set to the climatological profile of the 30–60°N latitude band for summer and the tropical a priori profile is set to the climatological profile of the 10–30°N latitude band for one year. It has been checked that the use of two different a priori and constraints does not induce discontinuities in the retrieved ozone fields. This reduces possible oscillations in the ozone profile induced by compensation effects during the retrieval procedure, especially in the tropics.

2.1.3 Validation

The IASI ozone product used in this study has been extensively characterized and validated using ozone-sondes (Keim et al., 2009; Dufour et al., 2012). Dufour et al. (2012) showed that the mean bias in the lower troposphere from the surface to 6 km is -2% (-0.38 DU) for typical mid-latitude measurements. In the mid-latitudes, the main difference between IASI and the ozone-sondes arises in the UTLS column (between 8 and 16 km) with a bias of 13.2% (6.3 DU) on average. In the tropics, the biases are larger: -6.2% (-1.5 DU) in the lower troposphere (between surface and 8 km) and 23.6% (6.1 DU) in the UTLS (between 11 and 20 km). As the present study is focused on the Mediterranean basin during summer and some modifications in the retrieval algorithm have been made, we performed a specific validation restricted to the summer period for the two WOUDC ozone-sondes stations located most closely to the Mediterranean (Madrid and Ankara). The number of available ozone-sondes profiles is 72 over the validation period (summers between 2007 and 2012). The same coincidence criteria ($\pm 1^\circ$ in longitude and latitude and 7 hours) as Dufour et al. (2012) have been used. The mean bias for the lower tropospheric column is -1.9% (-0.4 DU), similar to the one from Dufour et al. (2012). The mean bias for the UTLS column (16.5%, 5.0 DU) is slightly larger than the bias reported by Dufour et al. (2012) for an entire year for all the mid-latitudes ozone-sonde stations. Indeed, a larger bias for the summer season for this part of the atmosphere has already been noticed (see Fig. 12 in Dufour et al., 2012). Several hypotheses (coarse vertical resolution, spectroscopic and radiative transfer uncertainties) have been discussed by Dufour et al. (2012) to

explain this bias. We refer the reader to this paper for more details. In the present study, we make the choice to present ozone concentrations rather than columns. We consider ozone concentrations at 3 km (asl) and 10 km (asl). Table 1 gives the mean bias and error estimates (given by the root mean square of the difference between IASI and the ozone-sondes) at these two levels. Results are consistent with those derived for the lower tropospheric and UTLS columns as well as with the validation exercise reported in Dufour et al. (2012). It is worth noticed that some cautions have to be made when interpreting the ozone distributions derived from IASI observations. Due to the reduced vertical sensitivity and resolution of IASI, ozone concentrations retrieved at 3 km describe the ozone variability roughly from 2 to 8 km (lower/mid- troposphere) and ozone concentrations retrieved at 10 km the ozone variability from 5 to 14 km (upper troposphere/lower stratosphere) (Dufour et al., 2010). Moreover, the height of maximum sensitivity for one level (i.e. the atmospheric layer to which the measurement is the most representative) can vary significantly from one pixel to another. This may happen mainly in the vicinity of the coasts, where the thermal contrast, driving the sensitivity of the observations, can vary dramatically from a land to a sea pixel, leading to some discontinuity in the retrieved ozone fields as the atmospheric layers sounded preferentially may be different. One example of this arises in Fig. 3a in the Black Sea area.

2.2 Methodology to analyse tropospheric ozone over the Mediterranean

Our analyses are based on the morning overpasses of IASI for which the thermal conditions are more favorable to retrieve relevant information in the lower troposphere. The monthly and daily variations of ozone at 3 km and 10 km altitude during the summertime period are used. Monthly averages over the considered IASI observation period (2007-2012) are used as a reference to analyze the ozone variability and anomalies. In the following, averages over the 6 years period are named climatology by convenience even if 6 years period is too short to clearly address a climatological mean. A land/sea mask has been applied to calculate the averages only over the Mediterranean sea (Fig. 2). The role of the atmospheric dynamical processes for the tropospheric ozone distribution and its variability over the Mediterranean Basin is then assessed comparing ozone observations to meteorological reanalyses. The meteorological data used in this study are taken from the ECMWF ERA-Interim Analysis atmospheric model. It is characterised by a 12 hour 4D-Var data assimilation system, a $0.75^\circ \times 0.75^\circ$ horizontal resolution and 91 vertical layers (Dee et al., 2011). The meteorological parameters are taken at 12 UTC for this study. The 850 hPa geopotential is used as a proxy for describing the lower tropospheric horizontal transport. It allows the characterisation of the meteorological systems, their relative positions and strength as well as the induced flux direction. The 200 and 300 hPa potential vorticity (PV) fields are used as tracers of the (partial) stratospheric character of air masses and of vertical exchange processes. Indeed, stratospheric ozone rich air masses are characterized by large potential vorticity corresponding to enhanced vertical stability (Holton et al., 1992). This induces a positive vertical gradient of PV as well as of ozone in the UTLS. A positive

temporal correlation between ozone and PV can thus be interpreted as a dynamic control (control by
200 transport processes) of ozone concentrations, both due to the alternative presence of air masses with
varying tropopause height and stratospheric character, and due to subsidence of air from the UTLS
region down to the middle troposphere (e.g., Beekmann et al., 1994). In this study, the ozone con-
centrations observed by IASI at the 10 km level can be compared to the 200 hPa potential vorticity
to infer the dynamic control of the ozone concentration variability. The PV at 300 hPa turned out to
205 best describe vertical transport from the lower stratosphere down to the mid-troposphere, especially
when important subsidence is present. Note that potential vorticity at lower altitudes is less reliable
for such analysis due to the non-conservative character of PV in the troposphere induced by diabatic
processes (Holton et al., 1992). These contributions of ozone at the mid-troposphere are analysed
using IASI retrievals at 3 km.

210 **3 Summertime ozone spatio-temporal variability during the 2007-2012 period**

In this section, we analyze the variability of ozone over the Mediterranean basin at the lower (3 km)
and the upper (10 km) troposphere using six years of IASI observations. A month-to-month analy-
sis and daily ozone anomalies analyses with respect to the climatological evolution are conducted.
Results are discussed with respect to the associated meteorological conditions. Figure 3a shows the
215 mean ozone concentrations retrieved with IASI at 3 km over the Mediterranean Basin for the 6 sum-
mers (June, July and August) between 2007 and 2012. Larger ozone values are located at the Eastern
part of the Mediterranean basin. The 3 km ozone concentrations inferred from IASI range between
70 and 80 ppbv in this region, in agreement with in situ measurements made during summertime
periods (e.g., Kalabokas et al., 2013). At this altitude over the basin, a steep horizontal west/east
220 ozone gradient is observed, with greater concentrations eastward of 15E (by about 20 ppb) than
westward. The largest ozone values are observed over Turkey where the 300 hPa potential vorticity
is also the largest (Fig. 3b). The large PV values indicate an activation of the vertical exchanges
due to the presence of the trough in this region. The large vertical downward velocities at 500 hPa
eastward of 15°E (Fig. 3c) suggest that the downward vertical transport of ozone-enriched air masses
225 from the upper troposphere to the lower troposphere can explain the enhancement of ozone over the
Eastern Mediterranean basin in the lower troposphere. It should be noted that the downward vertical
transport actually takes place at the western flank of the high PV-streamer (Fig. 3b) as theoretically
expected from a dynamical point of view (Hoskins, 1985). Apart from the important role of sub-
sidence, the high probability of tropopause folds over the area should also be considered. This
230 phenomenon advects stratospheric air into the upper and middle troposphere. Tyrlis et al. (2014)
indicates a global "hot spot" of summertime tropopause fold activity over a sector between the east-
ern Mediterranean and Afghanistan, in the vicinity of the subtropical jet. According to a study of
Sprenger et al. (2007), a maximum in stratosphere-to-troposphere transport (STT) is identified at

the western flank of the stratospheric PV streamers which implies a co-location with the area of the
235 strongest subsidence. The observed ozone gradient over the Mediterranean is then mainly associated
to the pronounced subsidence over the Central and Eastern Mediterranean basin, arising from the di-
abatic convection over the Persian Gulf during the Indian monsoon. These results are in agreement
with previous studies based on in situ measurements (Kalabokas et al., 2013) and model analyses
(Zanis et al., 2014). In addition, it is worth noting that the western part of the basin is located down-
240 wind of the Atlantic ocean and influenced by advection of more pristine air masses (Fig. 3d). For
the Western basin, ozone enhancements occur over shorter time periods and are usually local events.
They can be explained by local dynamics such as sea breeze that can transport polluted air masses
over the sea (Velchev et al., 2011; Millan et al., 2000). The low sensitivity of IASI near the surface,
where these local processes arise, makes their observation difficult. Note that the West/East gradient
245 of ozone can be potentially reinforced by the Etesian winds in the lower troposphere, which transport
air masses from European continental areas. For comparison, we also analyze the ozone distribution
observed by IASI in the upper troposphere (10 km) during summer (Fig. 4). This comparison shows
that the ozone concentrations retrieved from IASI at 3 km (Fig. 3a) and at 10 km (Fig. 4) are clearly
uncorrelated and that IASI observations provide reliable information on the ozone spatial variability
250 in the lower and the upper troposphere. As expected, a North/South horizontal gradient is observed
in the upper troposphere (Fig. 4).

The large number of IASI observations available provides the opportunity to investigate the tem-
poral variability of ozone over the Mediterranean Basin at a interannual scale and on a monthly
basis. The monthly variability of ozone at the scale of the basin has been very little investigated
255 and satellite observations have not been exploited for this purpose to our knowledge. The temporal
variability of lower tropospheric ozone is driven by both the vertical and horizontal dynamics of the
troposphere. Indeed, our analysis suggests that vertical exchanges between the higher and the lower
troposphere lead to a maximum of the monthly mean 3 km ozone concentration in July (Fig. 5).
This lower tropospheric maximum is correlated to a 300 hPa potential vorticity maximum occur-
260 ring also in July (Fig. 6). The Pearson correlation coefficient between ozone concentrations at 3 km
(Fig. 5) and potential vorticity at 300 hPa (Fig. 6), calculated over the 3 summer months of the 6
considered years, is 0.99. The correlation is calculated from a 18 data points (6 years * 3 months).
The ozone maximum corresponds also to a 850 hPa geopotential maximum in July. Indeed, the
North African anticyclone is stronger in July with values larger than $15300 \text{ m}^2 \cdot \text{s}^{-2}$ (Fig. 7b) com-
265 pared to June (maximum values of $15100 \text{ m}^2 \cdot \text{s}^{-2}$, Fig. 7a) and August (maximum values of 15200
 $\text{m}^2 \cdot \text{s}^{-2}$, Fig. 7c). As well, the depression over the Eastern basin is deeper in July ($14200 \text{ m}^2 \cdot \text{s}^{-2}$,
Fig. 7a) than in June ($14400 \text{ m}^2 \cdot \text{s}^{-2}$, Fig. 7a) and in August ($14300 \text{ m}^2 \cdot \text{s}^{-2}$, Fig. 7c). This also
indicates that the North/South horizontal advection flux located between these two systems is more
pronounced during July, potentially leading to an additional enhancement of ozone concentrations
270 due to the transport of ozone enriched air masses from Europe. Tyrllis and Lelieveld (2013) have

shown that the strength of Etesian winds and of the subsidence over the Mediterranean basin are maximum in July and that these maxima were temporally very well correlated with the monsoon convection over northern India. As a consequence, the variability of ozone concentrations at 3 km height over the Mediterranean basin is characterized by a maximum in July. This feature seems fairly stable over different years (Fig. 5), nevertheless few anomalies with respect to the average behavior are also present. Especially during summer 2009, the monthly mean ozone concentration at 3 km height increases between June and August, with particularly low values for June and July (about 60 ppbv for June 2009 as compared to about 65 ppbv for the 2007-2012 June monthly ozone mean at 3 km). Summer 2008 also shows an anomaly compared to the climatology with a large ozone concentration at 3 km in June (about 69 ppbv compared to about 65 ppbv for the 2007-2012 June monthly mean of 3 km ozone). A detailed analysis provides a better understanding of how the dynamics controls the ozone concentrations over the Mediterranean basin. A day-to-day analysis of these anomalies is presented in the next section.

By comparison, we also present the interannual variations of summer monthly average concentrations at 10 km height, which is different compared to that at 3 km (Fig. 8). The monthly mean ozone in the upper troposphere decreases from June to August with a marked maximum in June (Fig. 8). This ozone decrease is related to the well known annual cycle of ozone that presents mid-latitude spring maximum at these altitudes. The interannual variability of upper tropospheric ozone is weak especially in July and August and the June to August concentration decreases persist over the six years.

4 Anomalies analysis : June 2008 and June/July 2009

In the 3 km ozone monthly variations presented in Fig. 5, two years (2008 and 2009) present anomalies compared to the climatological average between 2007 and 2012. During summer 2008, June ozone concentrations at 3 km are significantly larger than for the other years whereas during summer 2009, ozone concentrations increase progressively from June to August with unusual low ozone values in June and July. In this section, we present an analysis of the meteorological situation for the two specific years that explains the anomalies.

4.1 Case of June 2008

In order to explain the June 2008 positive ozone anomaly, we investigate the link between the synoptic meteorological conditions and the ozone daily variations for this month. Figure 9 shows that two high ozone events are observed by IASI at 3 km altitude: one around 10 June 2008 and another one between 20 June 2008 and 4 July 2008 (Fig. 9). The ozone concentrations averaged over the Mediterranean sea during these periods are about 72.5 ppbv, much more than the median value (64 ppbv) calculated over the 6 years period. For two days (1-2 July 2008), the ozone values

305 even exceed the 75% quartile (76 ppbv) calculated over all the ozone profiles measured over the basin. Studying separately the Eastern and the Western basin shows that the Eastern basin is the most affected. Ozone concentrations exceed 80 ppb during these periods and even exceed the 93% quartile for some days, whereas the ozone concentrations remain smaller than 70 ppb on average over the Western basin (not shown). These two events are well correlated to the 300 hPa potential
310 vorticity, which also presents two maxima for the same periods with values about 1 PVU over the Mediterranean basin (Fig. 10). The Pearson correlation coefficient between the 300 hPa potential vorticity and the 3 km ozone concentration time series is 0.87 for the month of June 2008. This suggests again that the large ozone amount observed in this case is related to the vertical exchanges with the upper troposphere. This is confirmed by the analysis of the daily Indian Monsoon Index
315 (IMI, <http://apdrc.soest.hawaii.edu/projects/monsoon/seasonal-monidx.html>) which indicates positive anomalies events of the diabatical convective activity over the Indian Ocean during the month of June 2008. In addition, the 3 km ozone concentration time series is also correlated with the 850 hPa geopotential time series, both time series being averaged over the entire basin. The Pearson correlation coefficient is about 0.85. Figure 11 shows the mean 850 hPa geopotential for the period
320 between 15 June 2008 and 7 July 2008. The Azores Anticyclone was stronger during this period compared to the mean situation between 2007 and 2012 (Fig. 7a). It was also located at higher latitudes. The ridge over the Western Mediterranean basin is then strengthened as well as the horizontal Etesian flux over the lower troposphere of the Central and Eastern Mediterranean basin. In addition, the low-pressure system located at the Eastern part of the basin was also deeper during this period
325 compared to the mean over the 6 years period, suggesting an intensification of the vertical subsidence of ozone rich air masses. This is also confirmed by larger vertical descending winds at 500 hPa for June 2008 compared to the climatological mean (relative difference of 14.3%).

4.2 Case of June and July 2009

As previously, we analysed the meteorological conditions and the daily ozone variations for June
330 and July 2009 (Fig. 12). A low ozone episode is observed by IASI between 9 and 25 June 2009 and the first half of July 2009, with 3 km ozone values below the median and even below the first quartile between 11 and 21 June 2009 (Fig. 12). The daily 300 hPa potential vorticity over the Mediterranean presents moderate values (0.6 PVU) and indicates a low vertical exchange activity (Fig. 13). The potential vorticity at 300 hPa is not correlated with the 3 km ozone time series for
335 June 2009 (Pearson correlation coefficient of 0.44). This suggests that vertical exchange is not the major driving force for the ozone variability at 3 km. Indeed, the IMI daily variation shows strong negative anomalies, indicating a lower diabatical convective activity than the climatological mean during June and July 2009. In order to investigate which other dynamical processes can play a key role in this low ozone value period, we examine the mean daily 850 hPa geopotential value over the
340 basin (Fig. 14). The Pearson correlation coefficient between the 3 km ozone observed by IASI and

the 850 hPa geopotential shows an anti-correlation with a value of -0.79. For this period, the low values of 3 km ozone concentrations are then associated with high values of 850 hPa geopotential (Fig. 14), whereas the high geopotential values was associated to large ozone values for June 2008. The difference between June 2008 and 2009 arises from the fact that the meteorological systems (high/low pressure structures) are not located at the same positions in June 2008 and 2009. Indeed, in 2009, the high pressure levels are positioned over North Africa and the low pressure levels are located over both the Atlantic and the central Europe (Fig. 15a). These positions lead to a lower tropospheric flux directed in the lower troposphere from the Atlantic Ocean to the Mediterranean Sea inducing horizontal advection of oceanic clean air masses over the Mediterranean, as it has been observed also during low-ozone concentration periods in the area (Kalabokas et al., 2008, 2013). This meteorological situation persists from the beginning of June to the middle of July 2009 (Fig. 15b) and mainly explains the low values of lower tropospheric ozone for June and July 2009.

5 Conclusions

Six years (2007-2012) of satellite observations from IASI have been used to analyse the spatial and the temporal ozone variability over the Mediterranean basin during summertime periods (June, July, August). IASI observations with more than 200000 ozone profiles per summer over the Mediterranean basin provide a unique dataset to investigate the intraseasonal variability of ozone in this region. The availability of the data since 2007 allows the characterization of the interannual ozone variability.

IASI ozone observations at 3 km and at 10 km height provide reliable information for characterizing the lower and the upper tropospheric ozone variability, respectively. In the lower troposphere, a steep West/East horizontal gradient over the basin is observed, in agreement with the summertime pool of high ozone concentrations over the Eastern Mediterranean, already reported in literature (e.g., Zanis et al., 2014). Vertical velocities at 500 hPa and 300 hPa potential vorticity (from ERA-Interim reanalysis) present similar pools of high values or gradients over the Eastern basin confirming the key role of the vertical exchanges in controlling the ozone concentrations in this region. Indeed, our analysis confirms that upper tropospheric air masses with high ozone concentrations are efficiently transported downward into the middle and lower troposphere and largely modify the ozone budget over the Central and Eastern Mediterranean basin. In the upper troposphere, the monthly analysis of IASI ozone observations shows a June maximum (with respect to July and August) related to the annual cycle of upper tropospheric ozone (spring maximum). In the lower troposphere, ozone concentrations exhibit a July maximum that is related mainly to the relative position and the intensification of the Azores anticyclone and the Middle Eastern depression associated to Indian summer monsoon in July. Over the six considered years, the temporal evolution of ozone during summer turns out to be fairly stable. Nevertheless, two ozone anomalies were detected: June 2008 that

presents high ozone concentrations compared to other years and June and July 2009 that presents unusual low ozone concentrations. The June 2008 anomaly is explained by an intensification of the vertical exchanges over the Eastern basin associated to stronger than usual anticyclonic conditions over the Mediterranean.

380 The June and July 2009 anomaly is explained by the position of a strong anticyclone over North Africa and of low pressure systems over the Atlantic and Central Europe that induce a transport of clean oceanic air masses over the Mediterranean. The relative position and the strength of the key meteorological systems (Azores anticyclone and Middle Eastern depression) are thus determinant factors for the ozone variability observed in the lower troposphere over the Mediterranean. In
385 conclusion, the use of new data sets, and namely IASI tropospheric ozone observations, allows reaffirming the hypothesis that downward transport of upper tropospheric air masses to the middle and lower troposphere is responsible for the large ozone values and controls their variability. The possibility of a daily analysis (due to the high sampling capability of IASI) also permits to show how horizontal fluxes (here the import of clean oceanic air masses over the basin) can perturb the mean
390 situation.

The impact of European emissions potentially connected to the Etesian winds has not been investigated here. Even if this impact is not dominant (Richards et al., 2013), it probably needs to be quantified more precisely. Recently, Safieddine et al. (2014) investigated this point using IASI ozone observations and regional WRF-CHEM simulations.

395 *Acknowledgements.* This study was supported by the French Space Agency CNES (project "IASI-TOSCA"). The IASI mission is a joint mission of Eumetsat and the Centre National d'Etudes Spatiales (CNES, France). The IASI L1 data are distributed in near real time by Eumetsat through the Eumetcast system distribution. The authors acknowledge the Ether French atmospheric database (<http://ether.ipsl.jussieu.fr>) for providing the IASI L1C and L2 data. The authors thank the Institut für Meteorologie und Klimaforschung (IMK), Karlsruhe Institute of Technology (KIT), Germany, for a licence to use the KOPRA radiative transfer model, and especially
400 M. Höpfner for his help to set up the code. The ozone-sonde data used in this study were provided by the World Ozone and Ultraviolet Data Centre (WOUDC). The authors thank all those responsible for the WOUDC measurements and archives for making the ozone-sonde data available. Clément Doche is grateful to Meteo-France for financial support. ECMWF ERA-Interim data used in this study have been obtained from the ECMWF data
405 server.

References

- Alpert, P., Price, C., Krichak, S. O., Ziv, B., Saaroni, H., Osetinsky, I., Barkan, J., and Kishcha, P.: Tropical tele-connections to the Mediterranean climate and weather, *Advances in Geosciences*, 2, 157-160, 2005.
- Anagnostopoulou, C., Zanis, P., Katragkou, E., Tegoulas, I., and Tolika, K.: Recent past and future patterns
410 of the Etesian winds based on regional scale climate model simulations, *Climate Dynamics*, 42(7-8), 1819-1836, 2014.
- Beekmann, M., Ancellet, G., and Mégie, G.: Climatology of tropospheric ozone in Southern Europe and its relation to potential vorticity, *J. Geophys. Res.* 99, 12841-12853, 1994.
- Beer, R., T. A. Glavich, and D. M. Rider: Tropospheric Emission Spectrometer for the Earth Observing Sys-
415 tem's Aura satellite, *Appl. Opt.*, 40, 2356-2367, 2001.
- Boynard, A., Clerbaux, C., Coheur, P.-F., Hurtmans, D., Turquety, S., George, M., Hadji-Lazaro, J., Keim, C., and Meyer-Arnek, J.: Measurements of total and tropospheric ozone from IASI: comparison with correlative satellite, ground-based and ozone-sonde observations, *Atmos. Chem. Phys.*, 9, 6255-6271, doi:10.5194/acp-9-6255-2009, 2009.
- 420 Camredon, M., and Aumont, B.: Modélisation de l'ozone et des photooxydants troposphériques. I. L'ozone troposphérique : production/consommation et régimes chimiques, *Pollution Atmosphérique*, 193, 2007.
- Clarisse, L., R'Honi, Y., Coheur, P.-F., Hurtmans, D., and Clerbaux, C.: Thermal infrared nadir observations of 24 atmospheric gases, *Geophys. Res. Lett.*, 38, L10802, doi:10.1029/2011GL047271, 2011.
- Clerbaux, C., Boynard, A., Clarisse, L., George, M., Hadji-Lazaro, J., Herbin, H., Hurtmans, D., Pommier, M.,
425 Razavi, A., Turquety, S., Wespes, C., and Coheur, P.-F.: Monitoring of atmospheric composition using the thermal infrared IASI/MetOp sounder, *Atmos. Chem. Phys.*, 9, 6041-6054, doi:10.5194/acp-9-6041-2009, 2009.
- Coheur, P.-F., Barret, B., Turquety, S., Hurtmans, D., Hadji-Lazaro, J., and Clerbaux, C.: Retrieval and characterization of ozone vertical profiles from a thermal infrared nadir sounder, *J. Geophys. Res.*, 110, D24303,
430 doi:10.1029/2005JD005845, 2005.
- Cuesta, J., Eremenko, M., Liu, X., Dufour, G., Cai, Z., Höpfner, M., von Clarmann, T., Sellitto, P., Foret, G., Gaubert, B., Beekmann, M., Orphal, J., Chance, K., Spurr, R., and Flaud, J.-M.: Satellite observation of lowermost tropospheric ozone by multispectral synergism of IASI thermal infrared and GOME-2 ultraviolet measurements over Europe, *Atmos. Chem. Phys.*, 13, 9675-9693, doi:10.5194/acp-13-9675-2013, 2013.
- 435 Dee, D. P., Uppala, S. M., Simmons, A. J., Berrisford, P., Poli, P., Kobayashi, S., Andrae, U., Balmaseda, M. A., Balsamo, G., Bauer, P., Bechtold, P., Beljaars, A. C. M., van de Berg, L., Bidlot, J., Bormann, N., Delsol, C., Dragani, R., Fuentes, M., Geer, A. J., Haimberger, L., Healy, S. B., Hersbach, H., Hólm, E. V., Isaksen, L., Kållberg, P., Köhler, M., Matricardi, M., McNally, A. P., Monge-Sanz, B. M., Morcrette, J.-J., Park, B.-K., Peubey, C., de Rosnay, P., Tavolato, C., Thépaut, J.-N. and Vitart, F., The ERA-Interim reanalysis:
440 configuration and performance of the data assimilation system. *Q.J.R. Meteorol. Soc.*, 137: 553-597. doi: 10.1002/qj.828, 2011.
- Delmas, R., Mégie, G. and Peuch, V.-H.: *Physique et chimie de l'atmosphère*, Ed. Belin, Coll. Echelles, 640, 2005.
- Dufour, G., Eremenko, M., Orphal, J., and Flaud, J.-M.: IASI observations of seasonal and day-to-day variations
445 of tropospheric ozone over three highly populated areas of China: Beijing, Shanghai, and Hong Kong,

- Atmos. Chem. Phys., 10, 3787–3801, doi:10.5194/acp-10-3787-2010, 2010.
- Dufour, G., Eremenko, M., Griesfeller, A., Barret, B., LeFlochoëñ, E., Clerbaux, C., Hadji-Lazaro, J., Coheur, P.-F., and Hurtmans, D.: Validation of three different scientific ozone products retrieved from IASI spectra using ozone-sondes, *Atmos. Meas. Tech.*, 5, 611-630, doi:10.5194/amt-5-611-2012, 2012.
- 450 Eremenko, M., Dufour, G., Foret, G., Keim, C., Orphal, J., Beekmann, M., Bergametti, G., and Flaud, J.-M.: Tropospheric ozone distributions over Europe during the heat wave in July 2007 observed from infrared nadir spectra recorded by IASI, *Geophys. Res. Lett.*, 35, L18805, doi:10.1029/2008GL034803, 2008.
- Fishman, J., Wozniak, A. E., and Creilson, J. K.: Global distribution of tropospheric ozone from satellite measurements using the empirically corrected tropospheric ozone residual technique: Identification of the regional aspects of air pollution, *Atmos. Chem. Phys.*, 3, 893–907, doi:10.5194/acp-3-893-2003, 2003.
- 455 Foret, G., Eremenko, M., Cuesta, J., Sellitto, P., Barré, J., Gaubert, B., Coman, A., Dufour, G., Liu, X., Joly, M., Doche, C., and Beekmann, M.: Ozone pollution: What can we see from space? A case study, *J. Geophys. Res. Atmos.*, 119, 8476–8499, doi:10.1002/2013JD021340.
- Fuhrer, J.: Ozone risk for crops and pastures in present and future climates, *Naturwissenschaften*, 96, 173-194, 460 2009.
- George, M., Clerbaux, C., Hurtmans, D., Turquety, S., Coheur, P.-F., Pommier, M., Hadji-Lazaro, J., Edwards, D. P., Worden, H., Luo, M., Rinsland, C., and McMillan, W.: Carbon monoxide distributions from the IASI/METOP mission: evaluation with other space-borne remote sensors, *Atmos. Chem. Phys.*, 9, 8317-8330, doi:10.5194/acp-9-8317-2009, 2009.
- 465 Holton, James R., *An introduction to dynamic meteorology*, third edition, Academic Press, Inc.San Diego, California, 1992.
- Hopfner, M., Blom, C. E., Echle, G., Glatthor, N., Hase, F., and Stiller, G.: Retrieval simulations for MIPAS-STR measurements, edited by: Smith, W. L., *IRS 2000: Current Problems in Atmospheric Radiation*; Proc. of the Internat. Radiation Symp., St. Petersburg, Russia, 24–29 July 2000 Hampton, Va., DEEPAK Publ., 470 2001.
- Hoskins, B. J., McIntyre, M. E., and Robertson, A. W.: On the use and significance of isentropic potential vorticity maps, *Q. J. Roy. Meteor. Soc.*, 111, 877-946, 1945.
- IPCC: *Climate Change 2007: The Physical Science Basis. Contribution of Working Group I to the Fourth Assessment Report of the Intergovernmental Panel on Climate Change* [Solomon, S., D. Qin, M. Manning, Z. Chen, M. Marquis, K.B. Averyt, M.Tignor and H.L. Miller (eds.)]. Cambridge University Press, Cambridge, United Kingdom and New York, NY, USA, 2007.
- 475 Jacob, D. J.: Heterogeneous chemistry and tropospheric ozone, *Atmos. Env.*, 34, 2131-2159, 2000.
- Jones, D. B. A., Bowman, K. W., Horowitz, L. W., Thompson, A. M., Tarasick, D. W., and Witte, J. C.: Estimating the summertime tropospheric ozone distribution over North America through assimilation of observations from the Tropospheric Emission Spectrometer, *J. Geophys. Res.*, 113, D18307, doi:10.1029/2007JD009341, 480 2008.
- Jonson, J. E., Sunder, J. K., and Tarrasón, L.: Model calculations of present and future levels of ozone and ozone precursors with a global and regional model, *Atmos. Environ.*, 35, 525-537, 2001.
- Kalabokas, P. D. and Repapis, C. C.: A climatological study of rural surface ozone in central Greece, *Atmos. Chem. Phys.*, 4, 1139–1147, doi:10.5194/acp-4-1139-2004, 2004.
- 485

- Kalabokas, P. D., Mihalopoulos, N., Ellul, R., Kleanthous, S., and Repapis, C. C.: An investigation of the meteorological and photochemical factors influencing the background rural and marine surface ozone levels in the Central and Eastern Mediterranean, *Atmos. Environ.*, 42, 7894–7906, 2008.
- 490 Kalabokas, P. D., Cammas, J.-P., Thouret, V., Volz-Thomas, A., Boulanger, D., and Repapis, C. C.: Examination of the atmospheric conditions associated with high and low summer ozone levels in the troposphere over the Eastern Mediterranean, *Atmos. Chem. Phys. Discuss.*, 13, 2457–2491, 2013.
- Keim, C., Eremenko, M., Orphal, J., Dufour, G., Flaud, J.-M., Hopfner, M., Boynard, A., Clerbaux, C., Payan, S., Coheur, P.-F., Hurtmans, D., Claude, H., Dier, H., Johnson, B., Kelder, H., Kivi, R., Koide, T., Lopez Bartolome, M., Lambkin, K., Moore, D., Schmidlin, F. J., and Stubi, R.: Tropospheric ozone from IASI: 495 comparison of different inversion algorithms and validation with ozone sondes in the northern middle latitudes, *Atmos. Chem. Phys.*, 9, 9329–9347, doi:10.5194/acp-9-9329-2009, 2009.
- Kulawik, S. S., Osterman, G., Jones, D. B. A., and Bowman, K. W.: Calculation of altitude-dependent Tikhonov constraints for TES nadir retrievals, *IEEE T. Geosci. Remote*, 44, 1334–1342, 2006.
- 500 Lelieveld, J., Berresheim, H., Borrmann, S., Crutzen, P. J., Dentener, F. J., Fischer, H., de Gouw, J., Feichter, J., Flatau, P., Heland, J., Holzinger, R., Korrmann, R., Lawrence, M., Levin, Z., Markowicz, K., Mihalopoulos, N., Minikin, A., Ramanathan, V., de Reus, M., Roelofs, G.-J., Scheeren, H. A., Sciare, J., Schlager, H., Schultz, M., Siegmund, P., Steil, B., Stephanou, E., Stier, P., Traub, M., Williams, J., and Ziereis, H.: Global air Pollution crossroads over the Mediterranean, *Science*, 298, 794–799, 2002.
- Levy, J. I., Carrothers, T. J., Tuomisto, J. T., Hammitt, J. K. and Evans, J. S.: Assessing the Public Health 505 Benefits of Reduced Ozone Concentrations, *Environ. Health Perspect.*, 109, 1215–1226, 2001.
- Li, Q., Jacob, D. J., Logan, J. A., Bey, I., Yantosca, R. M., Liu, H., Martin, R. V., Fiore, A. M., Field, B. D., Duncan, B. N., and Thouret, V.: A tropospheric ozone maximum over the Middle East, *Geophys. Res. Lett.*, 28, 3235–3238, doi:10.1029/2001GL013134, 2001.
- Liu, X., Chance, K. V., Sioris, C. E., Spurr, R. J. D., Kurosu, T. P., Martin, R. V., and Newchurch, M. J.: Ozone 510 profile and tropospheric ozone retrievals from Global Ozone Monitoring Experiment: Algorithm description and validation, *J. Geophys. Res.*, 110, D20307, doi:10.1029/2005JD006240, 2005.
- Liu, J. J., Jones, D. B. A., Worden, J. R., Noone, D., Parrington, M., and Kar, J.: Analysis of the summertime buildup of tropospheric ozone abundances over the Middle East and North Africa as observed by the Tropospheric Emission Spectrometer instrument, *J. Geophys. Res.*, 114, D05304, doi:10.1029/2008JD010993, 515 2009.
- Marenco, A., Thouret, V., Nédélec, P., Smit, H., Helten, M., Kley, D., Karcher, F., Simon, P., Law, K., Pyle, J., Poschmann, G., Von Wrede, R., Hume, C., and Cool, T.: Measurement of ozone water vapor by Airbus in-service aircraft: The MOZAIC airborne program, An overview, *J. Geophys. Res.*, 103, 25631–25642, doi:10.1029/98JD00977, 1998.
- 520 McPeters, R. D., Labow, G. J., and Logan, J. A.: Ozone climatological profiles for satellite retrieval algorithms, *J. Geophys. Res.*, 112, D05308, doi:10.1029/2005JD006823, 2007.
- Millan, M., Mantilla, E., Salvador, R., Carratala, A., Sanz, M.J., Alonso, L., Gangoiti, G., and Navazo, M.: Ozone cycles in the western Mediterranean basin: interpretation of monitoring data in complex coastal terrain, *Journal of Applied Meteorology*, 4, 487–507, 2000.
- 525 Nolle, M., Ellul, R., Heinrich, G., and Güsten, H.: A long-term study of background ozone concentrations in the

- central Mediterranean – diurnal and seasonal variations on the island of Gozo, *Atmos. Env.*, 36, 1391-1402, 2001.
- Prezerakos, NG: Does the extension of the Azores' anticyclone towards the Balkans really exist, *Arch Meteorol Geophys Bioclimatol Ser A* 33:217–227, 1984.
- 530 Richards, N. A. D., Arnold, S. R., Chipperfield, M. P., Miles, G., Rap, A., Siddans, R., Monks, S. A., and Hollaway, M. J.: The Mediterranean summertime ozone maximum: global emission sensitivities and radiative impacts, *Atmos. Chem. Phys.*, 13, 2331-2345, doi:10.5194/acp-13-2331-2013, 2013.
- Roelofs, G. J., Scheeren, H. A., Heland, J., Ziereis, H., and Lelieveld, J.: A model study of ozone in the eastern Mediterranean free troposphere during MINOS (Auhust 2001), *Atmos. Chem. Phys.*, 3, 1199-1210, 535 doi:10.5194/acp-3-1199-2003, 2003.
- Safieddine S., Clerbaux C., George M., Hadji-Lazaro J., Hurtmans D., Coheur P-F., Wespes C., Loyola D., Valks P., and Hao N.: Tropospheric ozone and nitrogen dioxide measurements in urban and rural regions as seen by IASI and GOME-2, *J. Geophys. Res.: Atmospheres* 118, 18, 10555-10566 - hal-00847335-, 2013.
- Safieddine, S., Boynard, A., Coheur, P-F., Hurtmans, D., Pfister, G., Quennehen, B., Thomas, J. L., Raut, J.-C., 540 Law, K. S., Klimont, Z., Hadji-Lazaro, J., George, M., and Clerbaux, C.: Summertime tropospheric ozone assessment over the Mediterranean region using the thermal infrared IASI/MetOp sounder and the WRF-Chem model, *Atmos. Chem. Phys. Discuss.*, 14, 12377-12408, doi:10.5194/acpd-14-12377-2014, 2014.
- Sprenger, Michael, Heini Wernli, and Michel Bourqui: Stratosphere–Troposphere Exchange and Its Relation to Potential Vorticity Streamers and Cutoffs near the Extratropical Tropopause, *J. Atmos. Sci.*, 64, 1587–1602, 545 doi: <http://dx.doi.org/10.1175/JAS3911.1>, 2007.
- Stiller, G. P.: The Karlsruhe optimized and precise radiative transfer algorithm (KOPRA), FZKA, 2000.
- Stohl, A., James, P., Forster, C., Spinchtinger, N., Marenco, A., Thouret, V., and Smit, H. G. J.: An extension of MOZAIC ozone climatologies using trajectory statistics, *J. Geophys. Res.*, 106, 27757-27768, 2001.
- Tyrlis, E. and Lelieveld, J.: Climatology and dynamics of the summer Etesian winds over the Eastern Mediterranean, *J. Atmos. Sci.*, doi:10.1175/JAS-D-13-035.1, in press, 2013.
- 550 Tyrlis, E., B. Škerlak, M. Sprenger, H. Wernli, G. Zittis, and J. Lelieveld: On the linkage between the Asian summer monsoon and tropopause fold activity over the eastern Mediterranean and the Middle East, *J. Geophys. Res. Atmos.*, 119, 3202–3221, doi:10.1002/2013JD021113, 2014.
- Velchev, K., Cavalli, F., Hjorth, J., Marmer, E., Vignati, E., Dentener, F., and Raes, F.: Ozone over the Western 555 Mediterranean Sea – results from two years of shipborne measurements, *Atmos. Chem. Phys.*, 11, 675–688, doi:10.5194/acp-11-675-2011, 2011
- Volz-Thomas, A., Beekmann, M., Derwent, D., Law, K., Lindskog, A., Prévôt, A., Roemer, M., Schultz, M., Schurath, U., Solberg, S., and Stohl, A.: Tropospheric Ozone and its Control, Towards Cleaner Air for Europe – Science, Tools and Applications, Chap. 3, Synthesis and Integration (S&I) Project, 2003.
- 560 WMO: International list of selected and supplementary ships. 3d ed. WMO 47 (WMO/OMM 47, TP. 18), 143 pp, 1957.
- Worden, H. M., Logan, J. A., Worden, J. R., Beer, R., Bowman, K., Clough, S. A., Eldering, A., Fisher, B. M., Gunson, M. R., Herman, R. L., Kulawik, S. S., Lampel, M. C., Luo, M., Megretskaia, I. A., Osterman, G. B., and Shephard, M. W.: Comparisons of Tropospheric Emission Spectrometer (TES) ozone profiles 565 to ozone-sondes: Methods and initial results, *J. Geophys. Res.*, 112, D03309, doi:10.1029/2006JD007258,

2007.

Worden, H. M., Bowman, K. W., Eldering, A., and Beer, R.: Satellite measurements of the clear sky greenhouse effect from tropospheric ozone, *Nat. Geosci.*, 1, 305–308, doi:10.1038/ngeo182, 2008.

570 Zanis, P., Hadjinicolaou, P., Pozzer, A., Tyrlis, E., Dafka, S., Mihalopoulos, N., and Lelieveld, J.: Summertime free-tropospheric ozone pool over the eastern Mediterranean/Middle East, *Atmos. Chem. Phys.*, 14, 115-132, doi:10.5194/acp-14-115-2014, 2014.

Zbinden, R. M., Thouret, V., Ricaud, P., Carminati, F., Cammas, J.-P., and Nédélec, P.: Climatology of pure tropospheric profiles and column contents of ozone and carbon monoxide using MOZAIC in the mid-northern latitudes (24° N to 50° N) from 1994 to 2009, *Atmos. Chem. Phys.*, 13, 12363-12388, doi:10.5194/acp-13-12363-2013, 2013.

575 Ziv, B., Saaroni, H., and Alpert, P.: The factors governing the summer regime of the eastern Mediterranean, *Int. J. Climatol.*, 24, 1859-1871, 2004.

Table 1. Mean relative bias and Root Mean Square of Errors (RMSE) of IASI ozone observations at 3 km and 10 km. They are derived from the comparison of IASI observations and ozone-sonde measurements at Madrid and Ankara over the summertime periods between 2007 and 2012 (see text for more details). Bias and RMSE are given in percent and in ppbv (in parenthesis).

| | Bias | RMSE |
|-------|-----------|---------|
| 3 km | -3.2 (2) | 16 (10) |
| 10 km | 15.8 (16) | 21 (21) |

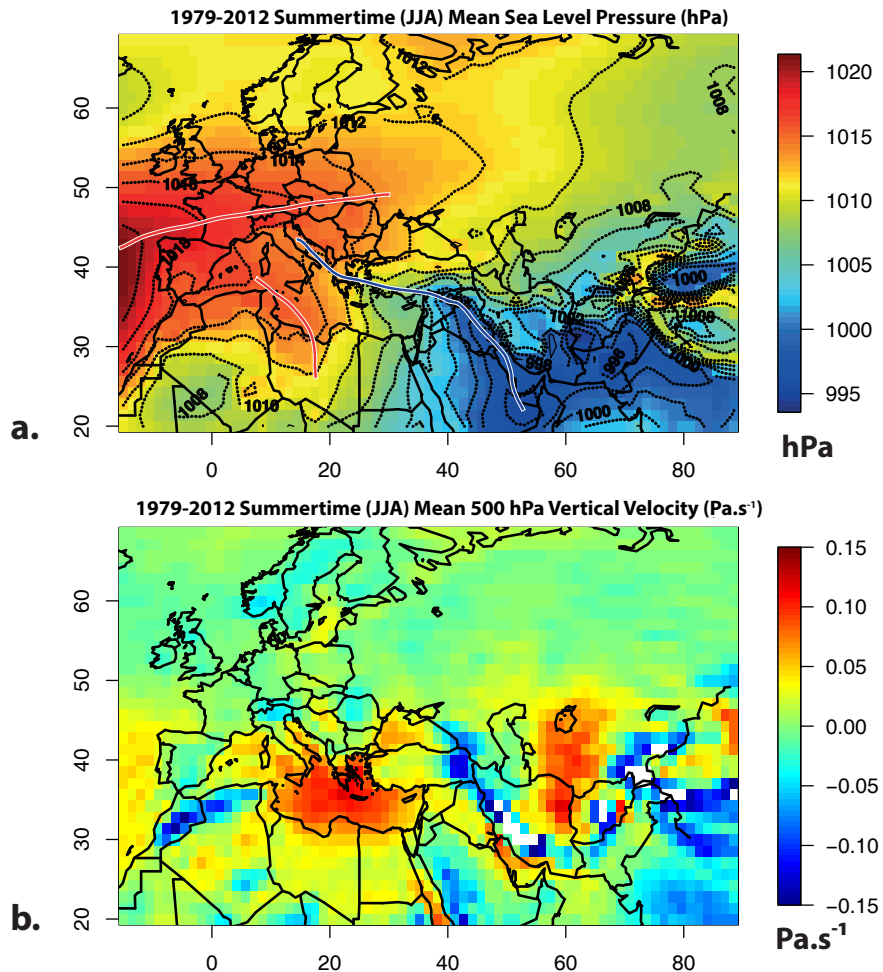


Fig. 1. 1979-2012 summertime (June, July and August) averages of meteorological variables taken from 12h ERA-Interim Reanalysis: (a) sea level pressure (hPa) (shades colours and black contour lines) – the red lines represents the high pressure ridges and the blue line the deep trough; (b) 500 hPa vertical velocity (Pa.s⁻¹) (white color corresponds to out of range values).



Fig. 2. Sea mask used to calculated ozone averages over the Mediterranean (blue dots). The dots represent the grid cells considered in the averages.

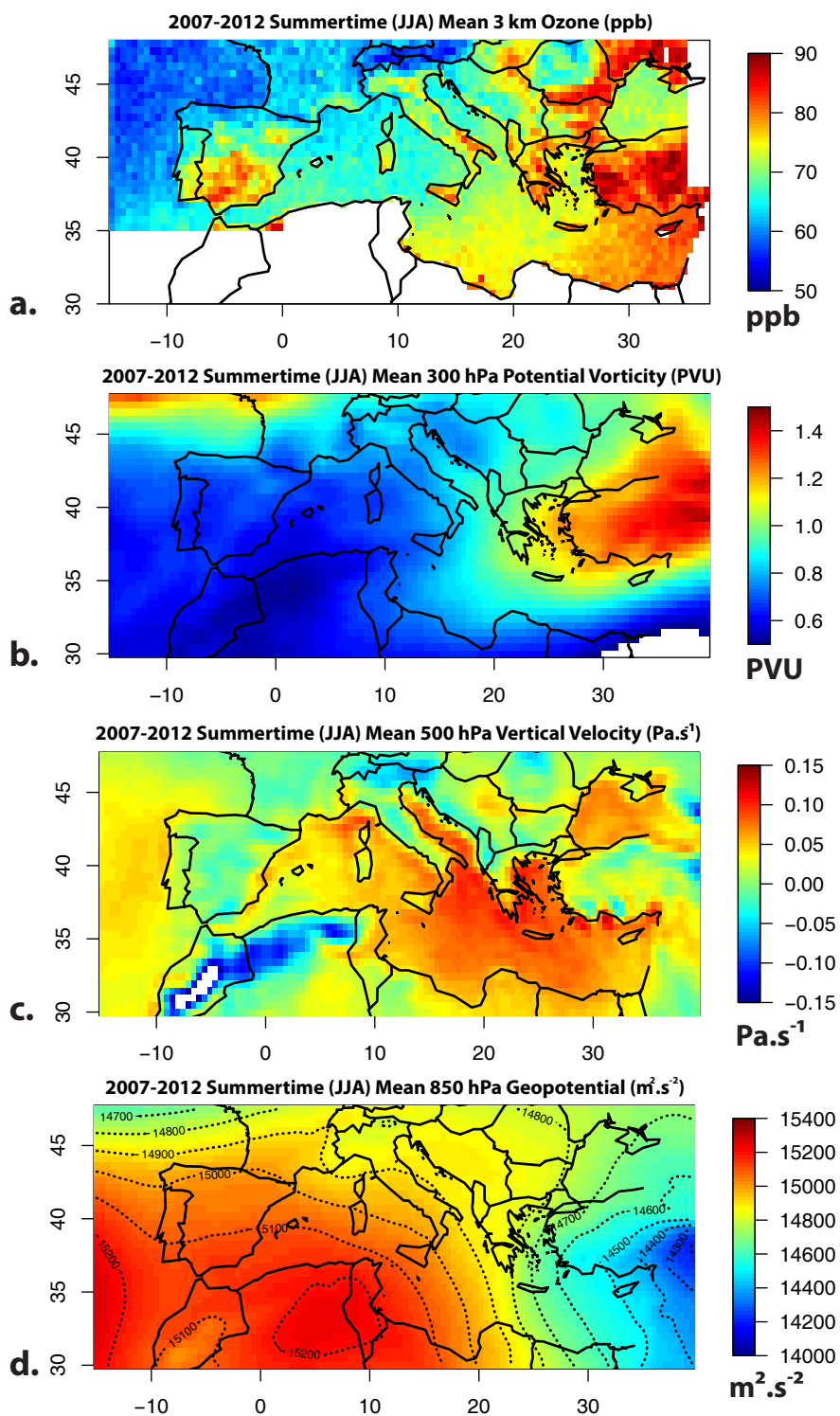


Fig. 3. 2007-2012 summertime (June, July, and August) average of ozone measured by IASI (morning overpasses) and meteorological variables taken from 12h ERA-Interim Reanalysis: (a) 3 km ozone concentration (ppb); (b) 300 hPa potential vorticity (PVU); (c) 500 hPa vertical velocity ($\text{Pa}\cdot\text{s}^{-1}$); (d) 850 hPa geopotential ($\text{m}^2\cdot\text{s}^{-2}$).

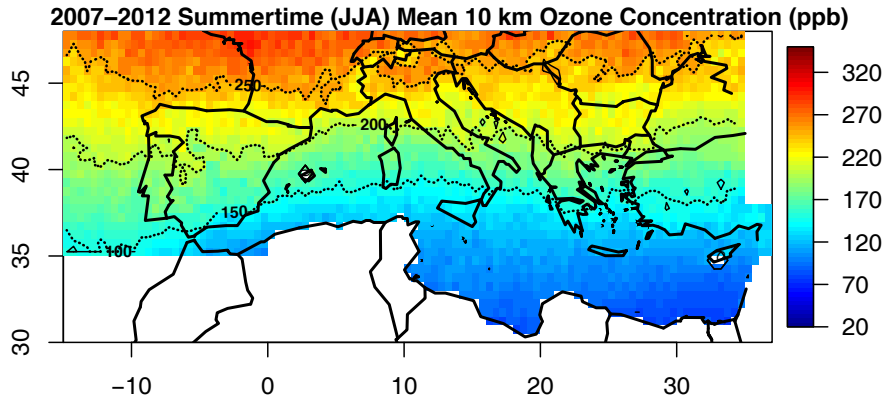


Fig. 4. 2007-2012 summertime (June, July, and August) average of 10 km ozone (ppb) measured by IASI (morning overpasses).

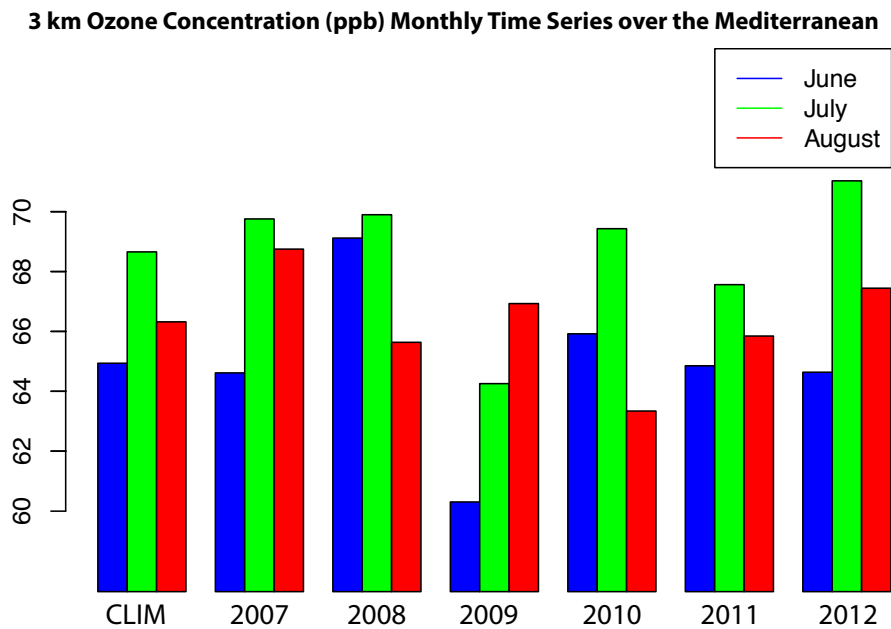


Fig. 5. Monthly means of 3 km ozone (ppb) measured by IASI during summertime period between 2007 and 2012 over the Mediterranean (IASI morning overpasses). Only the observations over the sea are considered in the averages. The monthly means referred as CLIM represent the averages over the entire period (2007-2012).

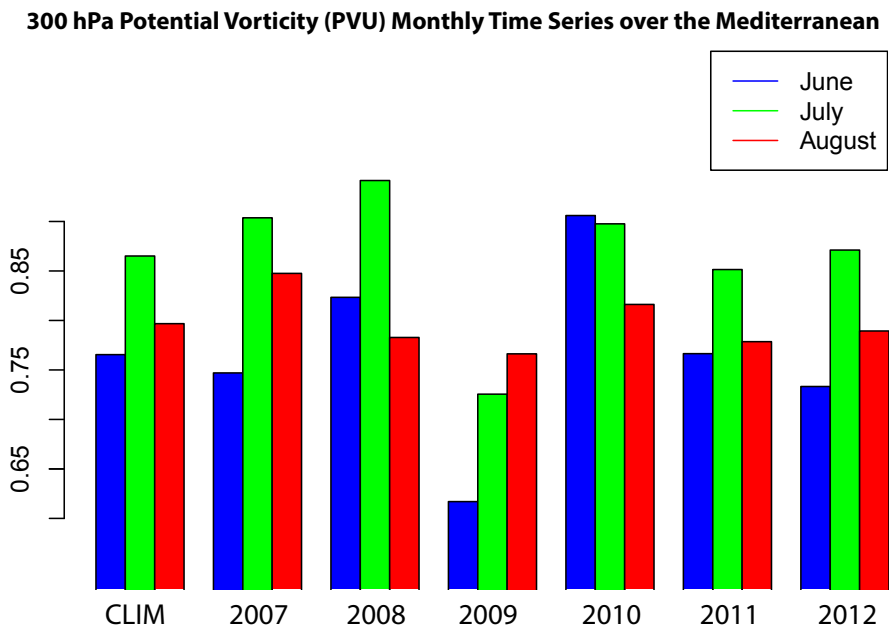


Fig. 6. Same as Fig. 5 for 300 hPa potential vorticity (PVU) taken from 12h ERA-Interim Reanalysis.

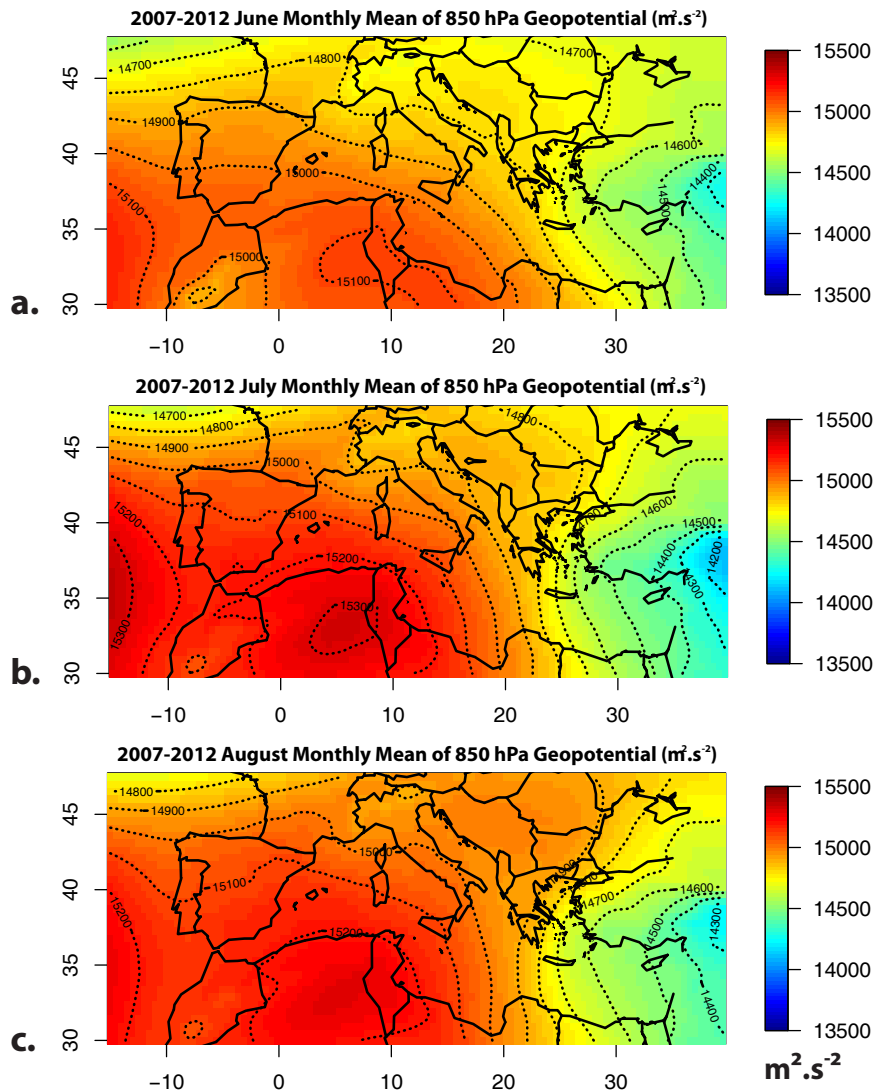


Fig. 7. 2007-2012 monthly mean of 850 hPa geopotential ($\text{m}^2.\text{s}^{-2}$) taken from 12h ERA-Interim Reanalysis (shade colours and black contour lines) for (a) June, (b) July and (c) August.

10 km Ozone Concentration (ppb) Monthly Time Series over the Mediterranean

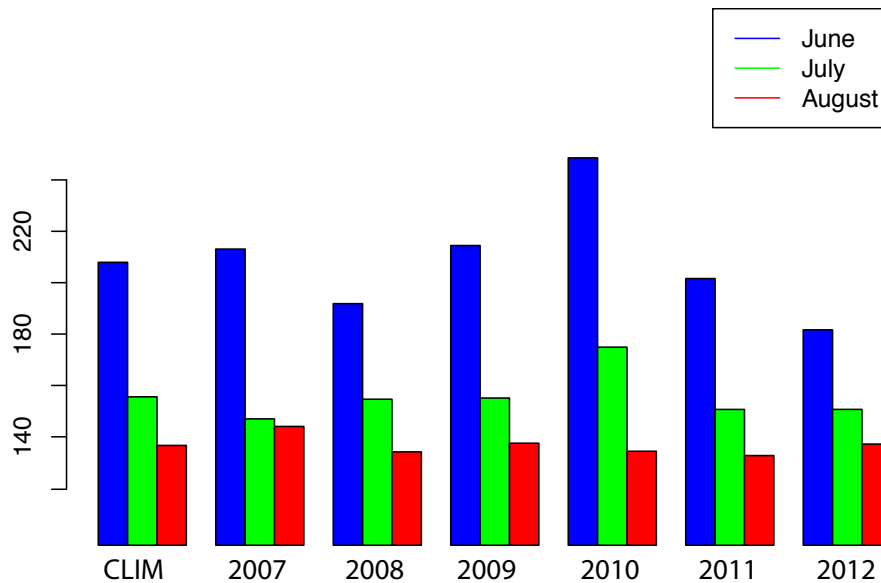


Fig. 8. Same as Fig. 5 for 10 km ozone measured by IASI.

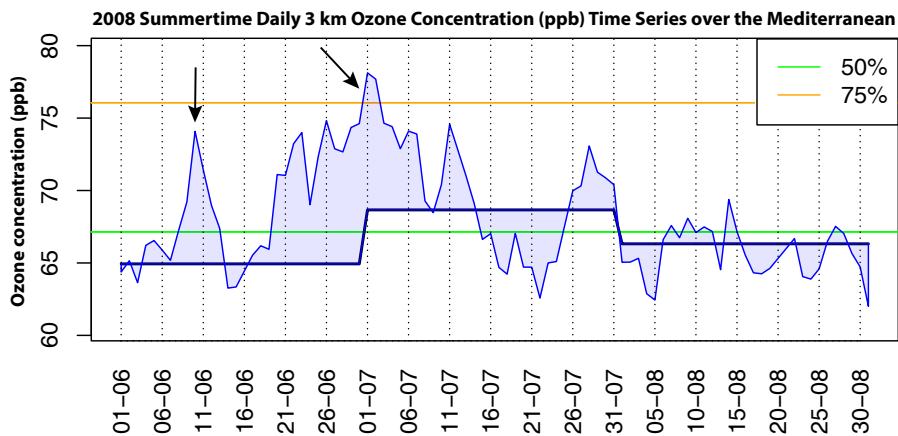


Fig. 9. 2008 summertime day-to-day mean 3 km ozone (ppb) time series measured with IASI (thin blue curve) over the Mediterranean (IASI morning overpasses). Only the observations over the sea are considered in the averages. 2007-2012 3 km ozone monthly mean are plotted in thick dark-blue curve. Horizontal coloured lines represent the 2007-2012 summertime (JJA) 3 km ozone quantiles for the data set of individual profiles.

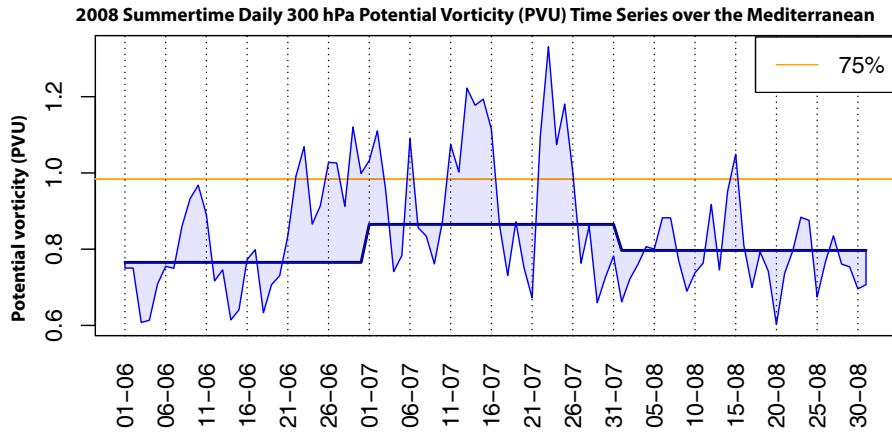


Fig. 10. Same as Fig. 9 for the 2008 summertime daily mean of 300 hPa potential vorticity (PVU) time series over the Mediterranean (12h ERA-Interim Reanalysis).

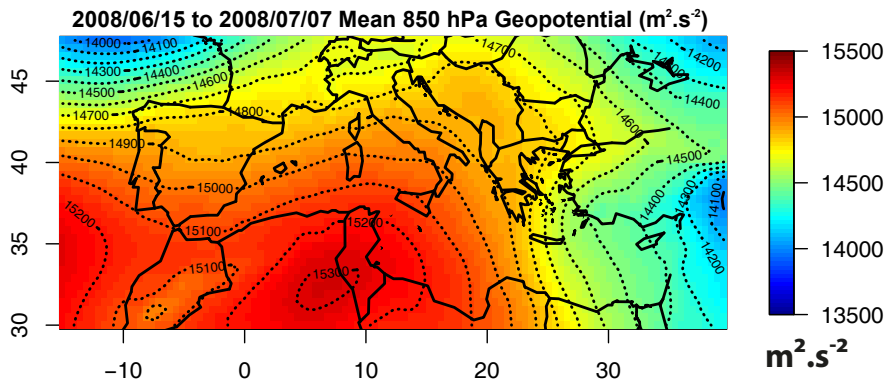


Fig. 11. Mean 850 hPa geopotential ($m^2.s^{-2}$) for the 15/06/2008-07/07/2008 period. The data are taken from 12h ERA-Interim Reanalysis.

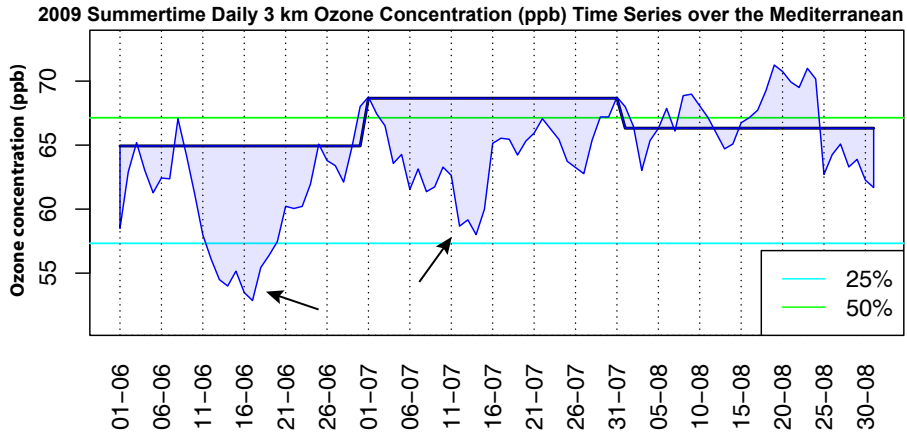


Fig. 12. Same as Fig. 9 for 2009 summer.

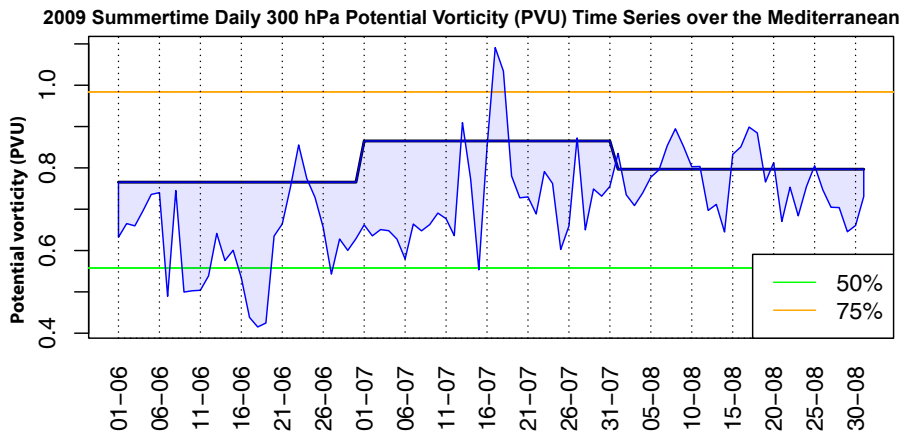


Fig. 13. Same as Fig. 10 for 2009 summer.

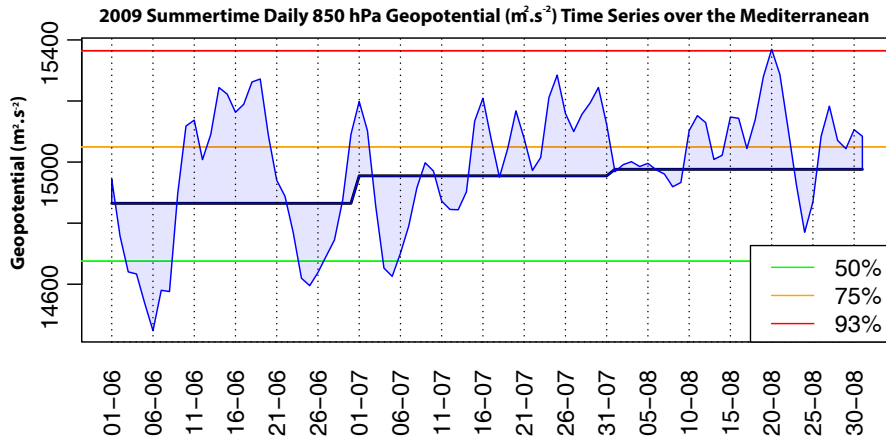


Fig. 14. Same as Fig. 13 for 850 hPa geopotential ($m^2.s^{-2}$) taken from 12h ERA-Interim Reanalysis.

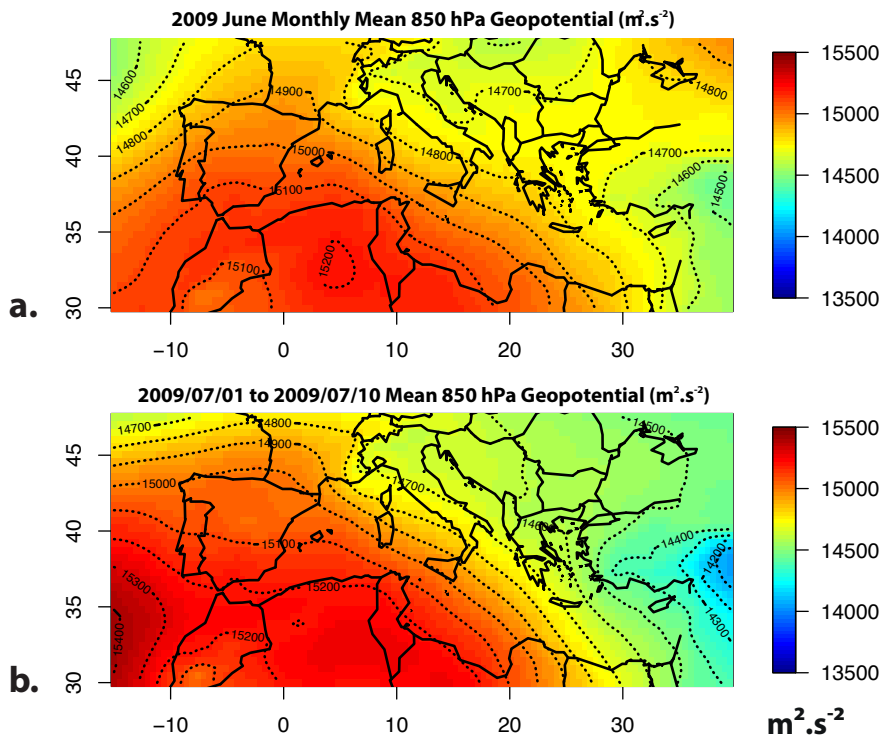


Fig. 15. Mean 850 hPa geopotential ($m^2.s^{-2}$) for (a) the June 2009 period and (b) the 01/07/2009-10/07/2009 period. Data are taken from the 12h ERA-Interim Reanalysis.